ACS APPLIED MATERIALS & INTERFACES

Research Article

www.acsami.org

Dual Amplified Electrochemical Immunosensor for Highly Sensitive Detection of *Pantoea stewartii* sbusp. *stewartii*

Yuan Zhao,[†,‡] Liqiang Liu,[†] Dezhao Kong,[†] Hua Kuang,*[,†] Libing Wang,[†] and Chuanlai Xu[†]

[†]State Key Lab of Food Science and Technology, School of Food Science and Technology, Jiangnan University, Wuxi, Jiangsu 214122, People's Republic of China

[‡]The Key Lab of Food Colloids and Biotechnology, Ministry of Education, School of Chemical and Materials Engineering, Jiangnan University, Wuxi, Jiangsu 214122, People's Republic of China

Supporting Information

ABSTRACT: Accurate and highly sensitive detection of *Pantoea stewartii* sbusp. *stewartii*-NCPPB 449 (PSS) is urgently required for international shipments due to tremendous agricultural economic losses. Herein, a dual amplified electrochemical sandwich immunosensor for PSS detection was developed, utilizing the good specificity and low cost of electrochemical immunoassay, the favorable conductivity and large specific surface area of gold nanoparticles (Au NPs), and the excellent catalytic ability of and horseradish peroxidase (HRP). A linear curve between current response and PSS concentration was established, and the limit of detection (LOD) was 7.8×10^3 cfu/mL, which is 20 times lower than that for conventional enzyme-linked immunosorbent assay (ELISA). This strategy is a useful approach for the highly sensitive detection of plant pathogenic bacterium.

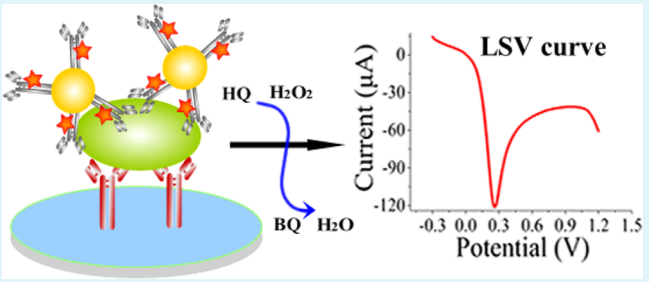

KEYWORDS: *Au NPs, electrochemical, immunosensor, PSS, sensitive detection*

1. INTRODUCTION

Pantoea stewartii sbusp. *stewartii*-NCPPB 449 (PSS) is a Gram-negative plant pathogenic bacterium that causes Stewart's vascular wilt in maize, and is classified as a quarantine organism in many countries.[1,2] Due to serious agricultural economic losses and the potential risk of transmission, a highly sensitive detection method for PSS is critical for international shipments. The main detection methods currently used are microbial assay (MA), ELISA and polymerase chain reaction (PCR).[3−5] Although these approaches are well-proven and accepted, complicated operations and false-positive signals as well as the low LODs have restricted the application of MA and ELISA.[6] In addition, PCR has high sensitivity, but requires expensive instruments.[2,6] A simple, accurate, highly sensitive and selective assay capable of detecting PSS is necessary for biodefense applications.

Electrochemical immunoassay has received more attention in recent years due to its specificity, portability, rapid detection and low cost.[7−12] Horseradish peroxidase (HRP) is an excellent electroactive label, which exhibits good stability and solubility, and is commonly introduced to catalyze substrates that produce quantitative electrochemical signals.[13−15] The concentration of PSS in maize is generally quite low in the early stage of the disease, thus there is a need to acquire amplified electrochemical signals and fabricate a disposable and portable electrochemical immunosensor for on-site monitoring in maize. Electroactive NPs have been successfully produced to amplify the electrochemical signals and improve the sensitivity of electrochemical immunosensors.[16−23] Au NPs with favorable conductivity, large specific surface area and high affinity for binding to amino-containing molecules not only allow the attachment of multiple electroactive labels but also accelerate electron transfer, which generates an amplified electrochemical signal.[14,15,24−26] In addition, the excellent biocompatibility of Au NPs retains the biological activity of the antibody, thus improving the analytical performance of the immunoassay.[22,26−29]

In this study, a simple and sensitive electrochemical immunoassay for PSS detection was for the first time developed using Au NPs and HRP for dual signal amplification, without significantly increasing the complexity of the procedures. HRP-labeled anti-PSS detection antibody (D-Ab-HRP) was prepared in comparison to previous reports of complex enzyme-labeled antigen procedures,[13] and then was attached to the surface of Au NPs. A sandwich immunosensor of capture anti-PSS antibody (C-Ab), PSS and D-Ab-HRP was established (Scheme 1). The current response of the immunosensors showed a linear relationship with the concentration of PSS, which ranged from 2.0×10^7 to 4.0×10^4 cfu/mL, and the limit of detection was as low as 0.78×10^4 cfu/mL (7.8×10^3 cfu/mL). Dual amplified electrochemical immunoassay took advantages of the extraordinary properties of Au NPs and the catalytic ability of

Received: September 8, 2014
Accepted: November 10, 2014
Published: November 10, 2014

 © 2014 American Chemical Society

Scheme 1. Schematic Illustration of Au NPs Amplified Electrochemical Immunoassay for PSS Detection

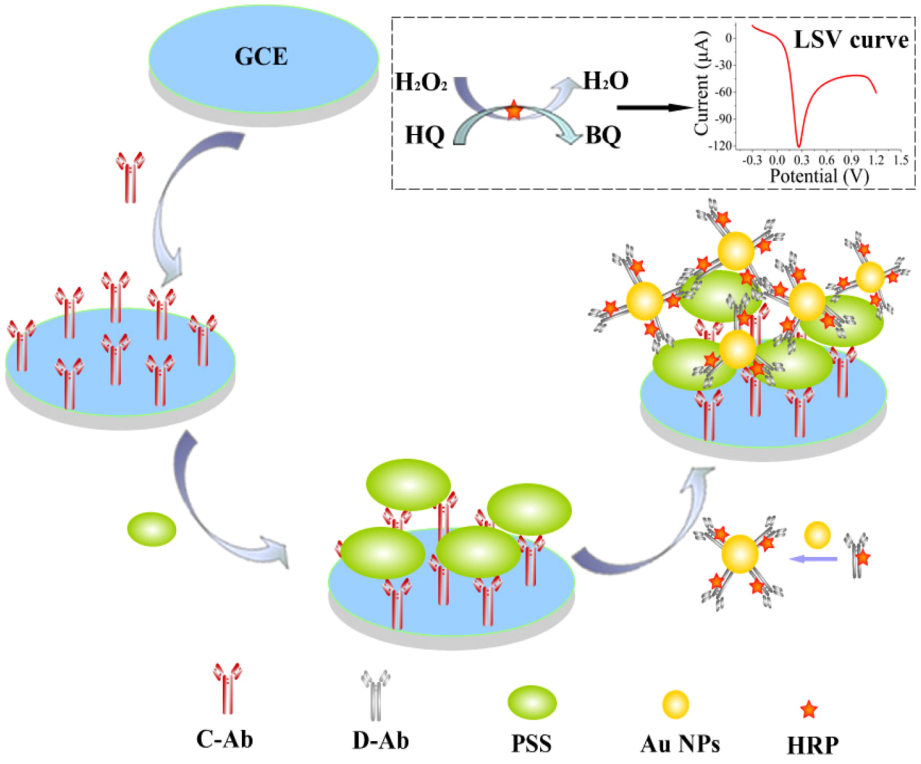

HRP, and achieved accurate and highly sensitive detection of the plant pathogenic bacterium.

2. EXPERIMENTAL SECTION

2.1. Materials and Reagents. Hydroquinone (HQ), *p*-aminobenzenesulfonic acid and phosphorus pentachloride were purchased from Shanghai Chemical Reagent. Hydrogen tetrachloroaurate trihydrate ($HAuCl_4 \cdot 3H_2O$), sodium citrate and HRP were purchased from Sigma-Aldrich. Bovine serum albumin (BSA) was obtained from Sunshine Biotechnology Co., Ltd. (Nanjing, China). All other chemicals were of analytical grade. Millipore-Q water was obtained using a Milli-Q device (18.2 MΩ, Millipore, Molsheim, France).

2.2. Preparation of D-Ab-HRP Labeled Au NPs. 0.2 mL of 10 mg/mL HRP solution was reacted with 0.2 mL of 0.06 M $NaIO_4$ at 4 °C. After 30 min, 0.2 mL of 0.16 M ethylene glycol was added to the mixture and the solution reacted for 30 min at room temperature. 0.2 mg of D-Ab was added to the above solution and the pH was carefully adjusted to around 9.0 using 0.05 M carbonate buffer (pH 10.0). After 24 h, 0.08 mL of 5 mg/mL $NaBH_4$ solution was added and the mixture reacted for 2 h at 4 °C. 0.08 mL of saturated $(NH_4)_2SO_4$ solution was added to the mixture and the mixture was kept at 4 °C for 1 h to obtain HRP-conjugated D-Ab. The mixtures were centrifuged at 2400*g* for 30 min, and the precipitant was cleaned twice using half-saturated $(NH_4)_2SO_4$ solution and resuspended in 0.01 M pH 7.4 phosphate buffered saline (PBS) solution with the final concentration of D-Ab at 2 μg/mL. The D-Ab-HRP conjugates were dialyzed in 0.01 M pH 7.4 PBS solution for 3 days to remove the dissociative ammonium ions, and were stored at 4 °C in the dark.

18 ± 2 nm Au NPs were synthesized by reducing $HAuCl_4 \cdot 3H_2O$ with sodium citrate.[30−32] 4 μL of 0.1 M K_2CO_3 solution was added to 1 mL of Au NPs solution, and then D-Ab-HRP solution was injected into the above mixture at the final concentration of 13 nM. After 1 h, 50 μL 10% BSA solution was added and blocked for 1 h. The conjugates were centrifuged at 5400*g* for 10 min and washed twice with PBS solution containing 2% (w/v) BSA, 2% (w/v) sucrose and 0.02% (w/v) sodium azide. The D-Ab-HRP-Au NPs conjugates were finally resuspended in 100 μL of PBS solution.

2.3. Immobilization of C-Ab onto Glassy Carbon Electrode (GCE). First, the GCE was carefully polished using 0.05 μm alumina slurry and washed with Millipore-Q water, followed sequentially by ultrasonic cleaning in Millipore-Q water and ethanol for 3 min each. The sulfated GCE was treated according to previous methods.[24] The GCE was scanned for 30 min in 50 mM *p*-aminobenzenesulfonic acid solution at 0.1 V/s between −0.5 and +0.5 V, and then immersed in 50 mM phosphorus pentachloride solution to activate the sulfonic groups, followed by washing and drying. Second, 5 μL of 10 μg/mL C-Ab was immobilized onto the surface of the GCE at 37 °C for 3 h. The C-Ab-GCE was rinsed three times with 0.01 M pH 7.0 phosphate buffered saline tween 20 (PBST) solution. Third, 5 μL of PBS solution containing 5% BSA was added to the surface of C-Ab-GCE and the redundant sites were blocked at 4 °C overnight. The C-Ab-GCE was washed three times with 0.01 M pH 7.0 PBST solution.

2.4. Fabrication of the Electrochemical Immunoassay. For PSS detection, the prepared C-Ab-GCE was immersed in different concentrations of PSS solution and incubated at room temperature for 1 h, followed by rinsing with 0.01 M pH 7.0 PBST solution and drying by N_2. Then, 5 μL of D-Ab-HRP-Au NPs was added to the surface of the electrode to combine with PSS for 1 h and the electrode was washed with 0.01 M pH 7.0 PBST solution three times. The sandwich structure of C-Ab-PSS-D-Ab was formed. 8 mL of pH 7.0 PBS solution containing the enzymatic substrate of 1.5 mM HQ and 2.0 mM H_2O_2 was added to the electrolytic cell. The linear sweep voltammetric (LSV) curves of the enzymatic products were recorded.

2.5. Instrumentation and Measurement. Electrochemical measurements and the electrochemical impedance spectroscopy (EIS) were performed on a three-electrode system of the CHI660D electrochemical workstation (Chenhua Instrument Company, Shanghai, China), in which the GCE was the working electrode, the Pt wire was the auxiliary electrode and a saturated calomel electrode was the reference electrode. EIS was measured in a solution of 5 mM $[Fe(CN)_6]^{3-}$ and 0.1 M KCl from 1×10^5 to 0.1 Hz with a pulse amplitude of 5 mV. The morphology of Au NPs was characterized using transmission electron microscopy (TEM, JEOL JEM-2100) operating at an acceleration voltage of 200 kV. UV/vis spectra were

dx.doi.org/10.1021/am506104r | ACS Appl. Mater. Interfaces 2014, 6, 21178−21183

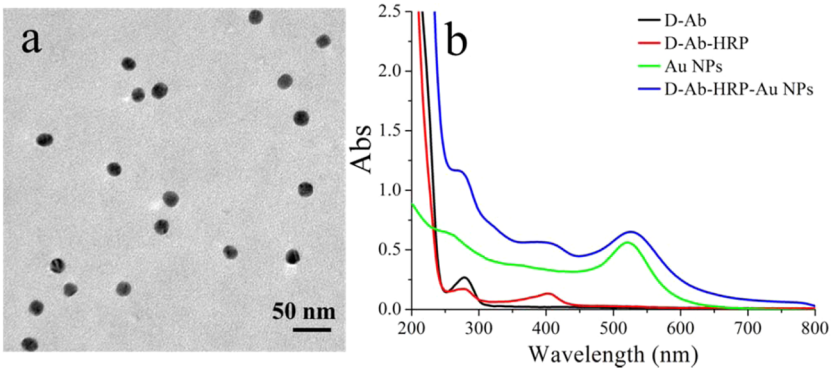

Figure 1. (a) TEM images of 18 ± 2 nm Au NPs; (b) UV−vis spectra of D-Ab, D-Ab-HRP, Au NPs and the conjugates of D-Ab-HRP-Au NPs.

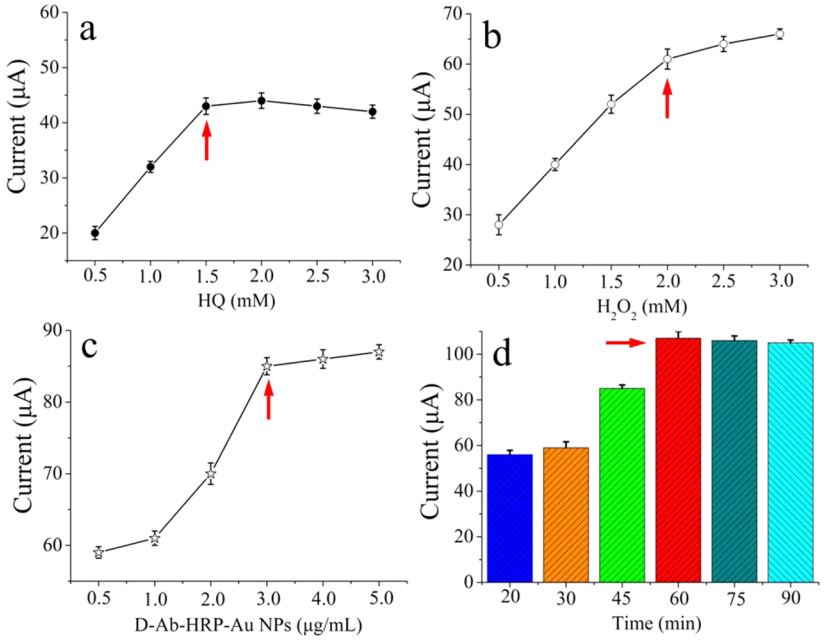

Figure 2. Current response of immunosensor in pH 7.0 PBS solution (a) at different HQ concentrations under 1 mM H_2O_2, 1 μg/mL D-Ab-HRP-Au and incubation for 45 min; (b) at different H_2O_2 concentrations under 1.5 mM HQ, 1 μg/mL D-Ab-HRP-Au NPs and incubation for 45 min; (c) at different D-Ab-HRP-Au NPs concentrations under 1.5 mM HQ, 2 mM H_2O_2 and incubation for 45 min; (d) at different incubation times under 1.5 mM HQ, 2 mM H_2O_2 and 1 μg/mL D-Ab-HRP-Au NPs.

measured by a UNICO 2100 PC UV/vis spectrophotometer and processed using Origin Lab software.

3. RESULTS AND DISCUSSION

3.1. Characterization of Au NPs and the Conjugates of D-Ab-HRP-Au NPs. In this study, an anti-PSS detection antibody (D-Ab) and an anti-PSS capture antibody (C-Ab) were prepared and paired in our laboratory. To achieve highly sensitive detection of PSS, Au NPs, as the supporter carrying HRP-labeled D-Ab, were fabricated.[33] As shown in Figure 1, the synthesized Au NPs of 18 ± 2 nm showed good dispersity, unique morphology and exhibited a localized surface plasmon resonance (LSPR) at 521 nm. D-Ab showed a UV absorption peak at 278 nm, whereas HRP-labeled D-Ab showed two obvious peaks at 278 and 402 nm, illustrating the successful modification of HRP on D-Ab according to the sodium periodate method. For D-Ab-HRP-Au NPs conjugates, not only the UV absorption of D-Ab and HRP was obtained but also the LSPR of Au NPs occurred to 5 nm red shift. The hydrodynamic sizes of Au NPs after modification showed a narrow size distribution (Figure S1, Supporting Information). No aggregation was observed from TEM images. These results showed Au NPs possessed good dispersity and good stability, indicating they can serve as an excellent biocompatible supporter to load D-Ab-HRP on the surface in the application. The average number of HRP-labeled anti-PSS detection antibody on each Au NP was calculated to be 4.1 ± 0.5 (Figure S2).

3.2. Optimization of the Experimental Conditions of the Immunoassay. The electrochemical immunoassay depended on the electrochemical features of HRP, which catalyzed the oxidation of HQ and H_2O_2. The enzymatic substrate concentration of HQ and H_2O_2, the amount of D-Ab-HRP-Au NPs and the incubation time all had an impact on the current response of the immunosensor. As shown in Figure 2a, under the same concentration of H_2O_2, D-Ab-HRP-Au and incubation time, the current response of the immunosensor increased with increasing concentration of HQ from 0.5 to 1.5 mM and tended to balance from 1.5 to 3.0 mM. The optimized concentration of HQ was 1.5 mM. Figure 2b shows the effect of H_2O_2 concentration on the current response of the immunosensor. 2.0 mM H_2O_2 was chosen as the optimum

concentration at which the maximum current was obtained. In the presence of 1.5 mM HQ and 2.0 mM H_2O_2, the catalytic current of the electrochemical immunoassay increased with increasing concentration of D-Ab-HRP-Au NPs conjugates from 0.5 to 3.0 μg/mL and an increase in incubation time from 20 to 60 min. However, there were no obvious changes at higher concentrations of D-Ab-HRP-Au NPs conjugates and longer incubation times.

3.3. Electrochemical Behaviors of Au NPs Amplified Immunosensors. The interface properties of surface-modified GCE were characterized through monitoring the changes of electron-transfer resistance (Figure S3, Supporting Information). In comparison with the small semicircle at high frequencies for bare GCE, C-Ab-GCE exhibited a higher resistance due to the poor conductivity of C-Ab, indicating the successful modification of C-Ab. Similarly, the resistance further increased after PSS combined with C-Ab on the electrode. The insulating C-Ab layer and PSS layer retarded the electron transfer, resulting in even higher resistance. Interestingly, when D-Ab-HRP-Au NPs conjugates were added onto the GCE surface, the resistance of the electrochemical immunosensors decreased, which was ascribed to the good conductivity for effective electron transfer.

Under the optimized detection conditions, the oxidation–reduction reaction between HQ and H_2O_2 catalyzed by HRP was promoted. As shown in the cyclic voltammetry (CV) curve of Figure 3, no redox response was observed for the bare GCE

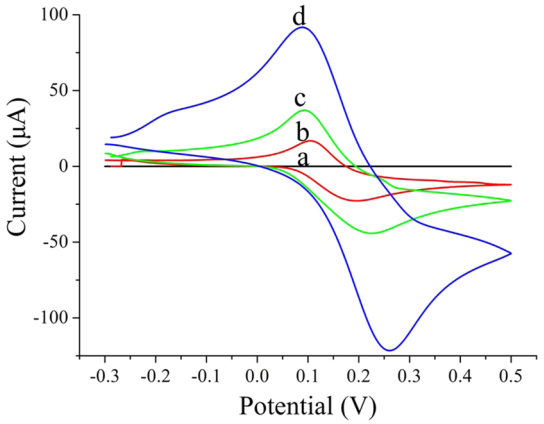

Figure 3. CV curves of (a) bare GCE in pH 7.0 PBS solution and (b,d) PSS-C-Ab-GCE in pH 7.0 PBS solution containing 1.5 mM HQ and 2 mM H_2O_2, without D-Ab-HRP (b), with D-Ab-HRP (c) and with D-Ab-HRP-Au NPs (d).

immersed in pH 7.0 PBS solution containing no HQ and H_2O_2. In comparison to the small redox peaks of the modified GCE immersed in pH 7.0 PBS solution containing 1.5 mM HQ and 2.0 mM H_2O_2, the modified GCE after incubation with D-Ab-HRP exhibited a higher current response, attributed to the excellent catalysis of HRP (Figure S4, Supporting Information). When D-Ab-HRP-Au NPs conjugates were immobilized on the surface of the PSS-C-Ab modified GCE, a substantial amplified current response was observed. The mechanism underlying the Au NPs amplified electrochemical signal can be ascribed to the good biocompatibility, excellent electron transfer and the superior specific surface area of Au NPs.[15,22,24,25] The favorable conductivity of Au NPs accelerated the electron transfer from enzymatic substrate to electrode. The high surface-to-volume of Au NPs enriched the amount of D-Ab-HRP, which further promoted the catalytic process and greatly improved the detection sensitivity of the immunoassay for the plant bacterium. However, the peak-to-peak separation showed a slight increase, which can be eliminated by optimizing the scanning rates and the concentration of different electrolyte solution, avoiding the polarization of electrodes and faultlessly polishing the electrodes.[28,34,35]

3.4. Analytical Performance of the PSS Electrochemical Immunoassay. A sandwich electrochemical immunoassay that depended on the highly specific molecular affinity of C-Ab, PSS and D-Ab was used to detect PSS. As shown in Figure 4, the linear sweep stripping voltammetric

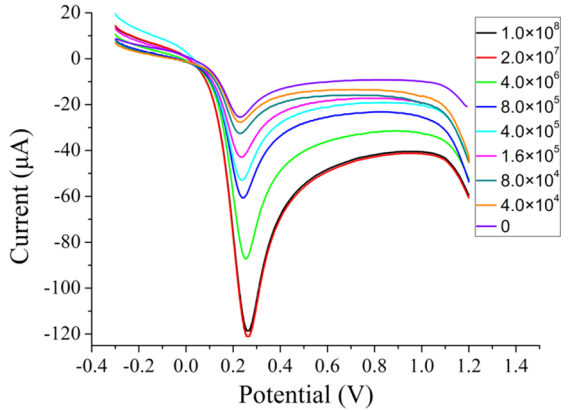

Figure 4. LSV curves of immunosensor at different PSS concentrations.

(LSV) curve of the C-Ab modified GCE after incubation with increasing concentrations of PSS and D-Ab-HRP-Au NPs conjugates showed an enhanced electrocatalytic current response in pH 7.0 PBS solution containing 1.5 mM HQ and 2.0 mM H_2O_2. A linear plot of the stripping peak current of the immunosensors versus the PSS concentration ranging from 2.0 × 10^7 to 4.0 × 10^4 cfu/mL was established with a correlation coefficient of 0.993 (Figure 5). The coincident peak potential of

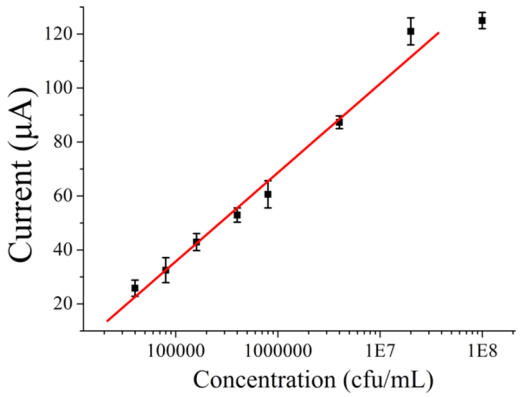

Figure 5. Calibration plots of the peak current of LSV and PSS concentration ranging from 2.0 × 10^7 to 4.0 × 10^4 cfu/mL.

the stripping peaks indicated good accuracy and reproducibility of the Au NPs amplified immunoassay. The LOD was down to 7.8 × 10^3 cfu/mL, which was calculated at a signal-to-noise ratio of 3σ (where σ was the standard deviation of the signal in a blank solution, see the Supporting Information). These results indicated that the proposed electrochemical immuno-

assay for PSS detection was highly sensitive and the detection limit was almost 20 times lower than that with ELISA (1.5×10^5 cfu/mL). In comparison to other methods depending on fluorescence signal or magnetic relaxation (Table S1, Supporting Information), dual amplified electrochemical sandwich immunoassay was free from oxygen, humidity and foreign species, and was simply operated, low cost, accurate and stable.

To evaluate the reliability of the Au NPs amplified immunoassay, spiked experiments were performed by quantifying the PSS concentration in corn seed soak solution. The recoveries for the spiked samples ranged from 90.6% to 107.5% (Table 1). The selectivity performance of the immunosensors

Table 1. Spiked Experiments for Different Concentrations of PSS

spiked concentration (cfu/mL)	detected concentration (cfu/mL)	recovery (%)
1.0×10^7	9.2×10^6	92.5 ± 2.4
2.0×10^6	1.8×10^6	90.6 ± 1.7
4.0×10^5	4.3×10^5	107.5 ± 3.4
8.0×10^4	8.5×10^4	106.3 ± 2.6

was studied using another four types of plant pathogenic bacteria at a concentration of 1.0×10^7 cfu/mL, and included *Burkholderia glumae* (NCPPB 2391), Rice bacterial leaf streak pathogen (NCPPB 1585), Rice bacterial *Cercospora* leaf spot pathogen (NCPPB 2844) and Crucifer black spot pathogen (NCPPB 1820). As illustrated in Figure 6, the current response

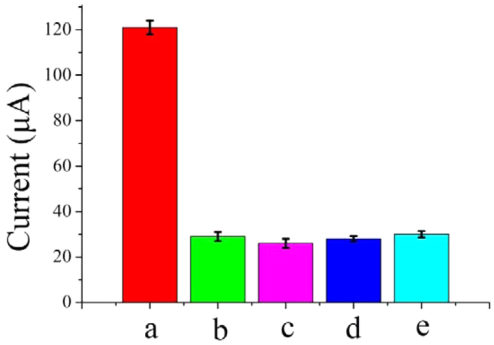

Figure 6. Evaluation of the cross-reactivity of electrochemical immunosensor at different target analytes. (a) PSS, (b) *Burkholderia glumae*, (c) Rice bacterial leaf streak pathogen, (d) Rice bacterial *Cercospora* leaf spot pathogen and (e) Crucifer black spot pathogen.

of electrochemical immunosensors for the other four target analytes was much smaller than that of PSS, which was mainly due to the weak redox reaction between HQ and H_2O_2 without the catalysis of HRP. Besides specificity, the regeneration and stability of electrochemical immunosensors were also important criterions in the real applications. The current response of sensors was investigated by detecting three different concentrations of PSS before and after elution (Figure S5, Supporting Information). There were almost no cross-impacts between different concentrations of PSS, and the current signal was easily recovered to the original current response of bare GCE. Furthermore, no obvious changes for CV curves were observed with 2 to 20 h (Figure S6, Supporting Information), illustrating the good stability of electrochemical sensors. These results showed that the Au NPs amplified electrochemical immunoassay has potential in real applications.

4. CONCLUSIONS

In summary, a dual amplified electrochemical immunoassay was developed for highly sensitive detection of PSS, utilizing the favorable conductivity and large specific surface area of Au NPs and the excellent catalytic ability of HRP. With a sandwich enzyme-based immunoassay format, the LOD for PSS detection was down to 7.8×10^3 cfu/mL, which increased the detection sensitivity by 20-fold compared with conventional ELISA. The biocompatible recognition and amplified signal provides a useful way to fabricate nanomaterials-driven electrochemical immunosensors for the highly sensitive and multiple plant pathogenic bacteria detection, which were critical on the way for achieving on-site monitoring of maize.

■ ASSOCIATED CONTENT

Supporting Information

Hydrodynamic sizes of Au NPs and the conjugates of D-Ab-HRP-Au NPs, detail calculation of antibody number on Au NPs by UV spectra, changes of electrochemical impedance spectroscopy of modified electodes, detail schematic illustration, LSV curves of C-Ab modified GCE for PSS detection and table of the comparison of LODs based on various methods. This material is available free of charge via the Internet at http://pubs.acs.org.

■ AUTHOR INFORMATION

Corresponding Author

*H. Kuang. E-mail: kuangh@jiangnan.edu.cn.

Notes

The authors declare no competing financial interest.

■ ACKNOWLEDGMENTS

This work is financially supported by the Key Programs from MOST (2012BAC01B07, 2012BAK17B10, 2012BAD29B04).

■ REFERENCES

(1) Roper, M. C. *Pantoea stewartii* subsp. *stewartii*: Lessons Learned From a Xylem-dwelling Pathogen of Sweet Corn. *Mol. Plant Pathol.* **2011**, *12*, 628−637.

(2) Zhang, F.; Zou, M.; Chen, Y.; Li, J.; Wang, Y.; Qi, X.; Xue, Q. Lanthanide-Labeled Immunochromatographic Strips for the Rapid Detection of *Pantoea stewartii* subsp. *stewartii*. *Biosens. Bioelectron.* **2014**, *51*, 29−35.

(3) Zhang, F.; Li, J.; Zou, M.; Chen, Y.; Wang, Y.; Qi, X. Simultaneous Detection of *Clavibacter michiganensis* subsp. *nebraskensis* and *Pantoea stewartii* subsp. *stewartii* Based on Microsphere Immunoreaction. *J. Biomol. Screening* **2013**, *18*, 474−480.

(4) Thapa, S. P.; Park, D. H.; Wilson, C.; Hur, J. H.; Lim, C. K. Multiplex PCR Assay for the Detection of *Pantoea stewartii* subsp. *stewartii* using Species-Specific Genetic Markers. *Australas. Plant Pathol.* **2012**, *41*, 559−564.

(5) Wensing, A.; Zimmermann, S.; Geider, K. Identification of the Corn Pathogen *Pantoea stewartii* by Mass Spectrometry of Whole-Cell Extracts and Its Detection with Novel PCR Primers. *Appl. Environ. Microbiol.* **2010**, *76*, 6248−6256.

(6) Chen, Y.; Zou, M.; Wang da, N.; Li, Y.; Xue, Q.; Xie, M.; Qi, C. An Immunosensor Based on Magnetic Relaxation Switch and Polystyrene Microparticle-induced Immune Multivalency Enrichment System for the Detection of *Pantoea stewartii* subsp. *stewartii*. *Biosens. Bioelectron.* **2013**, *43*, 6−11.

(7) Lin, D.; Wu, J.; Ju, H.; Yan, F. Signal Amplification for Electrochemical Immunosensing by in Situ Assembly of Host-Guest Linked Gold Nanorod Superstructure on Immunocomplex. *Biosens. Bioelectron.* **2013**, *45*, 195−200.
(8) Lin, D.; Wu, J.; Wang, M.; Yan, F.; Ju, H. Triple Signal Amplification of Graphene Film, Polybead Carried Gold Nanoparticles as Tracing Tag and Silver Deposition for Ultrasensitive Electrochemical Immunosensing. *Anal. Chem.* **2012**, *84*, 3662−3668.
(9) Yu, X.; Li, Y.; Wu, J.; Ju, H. Motor-based Autonomous Microsensor for Motion and Counting Immunoassay of Cancer Biomarker. *Anal. Chem.* **2014**, *86*, 4501−4507.
(10) Guo, A.; Wu, D.; Ma, H.; Zhang, Y.; Li, H.; Du, B.; Wei, Q. An Ultrasensitive Enzyme-Free Electrochemical Immunosensor for CA125 using Au@Pd Core-Shell Nanoparticles as Labels and Platforms for Signal Amplification. *J. Mater. Chem. B* **2013**, *1*, 4052−4058.
(11) Martic, S.; Gabriel, M.; Turowec, J. P.; Litchfield, D. W.; Kraatz, H. B. Versatile Strategy for Biochemical, Electrochemical and Immunoarray Detection of Protein Phosphorylations. *J. Am. Chem. Soc.* **2012**, *134*, 17036−17045.
(12) Yang, L.; Zhao, H.; Fan, S.; Deng, S.; Lv, Q.; Lin, J.; Li, C. P. Label-Free Electrochemical Immunosensor Based on Gold-Silicon Carbide Nanocomposites for Sensitive Detection of Human Chorionic Gonadotrophin. *Biosens. Bioelectron.* **2014**, *57*, 199−206.
(13) Zhang, J.; Lei, J.; Xu, C.; Ding, L.; Ju, H. Carbon Nanohorn Sensitized Electrochemical Immunosensor for Rapid Detection of Microcystin-LR. *Anal. Chem.* **2010**, *82*, 1117−1122.
(14) Ambrosi, A.; Airo, F.; Merkoci, A. Enhanced Gold Nanoparticle based ELISA for a Breast Cancer Biomarker. *Anal. Chem.* **2010**, *82*, 1151−1156.
(15) Zhao, J.; Zhang, Y.; Li, H.; Wen, Y.; Fan, X.; Lin, F.; Tan, L.; Yao, S. Ultrasensitive Electrochemical Aptasensor for Thrombin based on the Amplification of Aptamer-AuNPs-HRP Conjugates. *Biosens. Bioelectron.* **2011**, *26*, 2297−2303.
(16) Zong, C.; Wu, J.; Wang, C.; Ju, H.; Yan, F. Chemiluminescence Imaging Immunoassay of Multiple Tumor Markers for Cancer Screening. *Anal. Chem.* **2012**, *84*, 2410−2415.
(17) Wang, L.; Lei, J.; Ma, R.; Ju, H. Host-Guest Interaction of Adamantine with a Beta-Cyclodextrin-Functionalized AuPd Bimetallic Nanoprobe for Ultrasensitive Electrochemical Immunoassay of Small Molecules. *Anal. Chem.* **2013**, *85*, 6505−6510.
(18) Wan, Y.; Wang, Y.; Wu, J.; Zhang, D. Graphene Oxide Sheet-Mediated Silver Enhancement for Application to Electrochemical Biosensors. *Anal. Chem.* **2011**, *83*, 648−653.
(19) Chen, L.; Zhang, X.; Zhou, G.; Xiang, X.; Ji, X.; Zheng, Z.; He, Z.; Wang, H. Simultaneous Determination of Human Enterovirus 71 and Coxsackievirus B3 by Dual-Color Quantum Dots and Homogeneous Immunoassay. *Anal. Chem.* **2012**, *84*, 3200−3207.
(20) Jie, G.; Yuan, J. Novel Magnetic Fe_3O_4@CdSe Composite Quantum Dot-based Electrochemiluminescence Detection of Thrombin by a Multiple DNA Cycle Amplification Strategy. *Anal. Chem.* **2012**, *84*, 2811−2817.
(21) Wang, L.; Chen, W.; Xu, D.; Shim, B. S.; Zhu, Y.; Sun, F.; Liu, L.; Peng, C.; Jin, Z.; Xu, C.; Kotov, N. A. Simple, Rapid, Sensitive, and Versatile SWNT-Paper Sensor for Environmental Toxin Detection Competitive with ELISA. *Nano Lett.* **2009**, *9*, 4147−4152.
(22) Pondman, K. M.; Maijenburg, A. W.; Celikkol, F. B.; Pathan, A. A.; Kishore, U.; Haken, B. t.; ten Elshof, J. E. Au Coated Ni Nanowires with Tuneable Dimensions for Biomedical Applications. *J. Mater. Chem. B* **2013**, *1*, 6129−6136.
(23) Wang, Y.; Zhang, Y.; Su, Y.; Li, F.; Ma, H.; Li, H.; Du, B.; Wei, Q. Ultrasensitive Non-Mediator Electrochemical Immunosensors using Au/Ag/Au Core/Double Shell Nanoparticles as Enzyme-Mimetic Labels. *Talanta* **2014**, *124*, 60−66.
(24) Kuang, H.; Chen, W.; Xu, D.; Xu, L.; Zhu, Y.; Liu, L.; Chu, H.; Peng, C.; Xu, C.; Zhu, S. Fabricated Aptamer-based Electrochemical "signal-off" Sensor of Ochratoxin A. *Biosens. Bioelectron.* **2010**, *26*, 710−716.
(25) Zhang, Q.; Chen, X.; Tu, F.; Yao, C. Ultrasensitive Enzyme-Free Electrochemical Immunoassay for Free Thyroxine Based on Three Dimensionally Ordered Macroporous Chitosan-Au Nanoparticles Hybrid Film. *Biosens. Bioelectron.* **2014**, *59*, 377−383.
(26) Kavosi, B.; Hallaj, R.; Teymourian, H.; Salimi, A. Au Nanoparticles/PAMAM Dendrimer Functionalized Wired Ethyleneamine-Viologen as Highly Efficient Interface for Ultra-Sensitive Alpha-Fetoprotein Electrochemical Immunosensor. *Biosens. Bioelectron.* **2014**, *59*, 389−396.
(27) Wang, L.; Jia, X.; Zhou, Y.; Xie, Q.; Yao, S. Sandwich-Type Amperometric Immunosensor for Human Immunoglobulin G Using Antibody-Adsorbed Au/SiO_2 Nanoparticles. *Microchim. Acta* **2010**, *168*, 245−251.
(28) Yan, M.; Zang, D. J.; Ge, S. G.; Ge, L.; Yu, J. H. A Disposable Electrochemical Immunosensor Based on Carbon Screen-Printed Electrodes for the Detection of Prostate Specific Antigen. *Biosens. Bioelectron.* **2012**, *38*, 355−361.
(29) Lv, X.; Ge, W.; Li, Q.; Wu, Y.; Jiang, H.; Wang, X. Rapid and Ultrasensitive Electrochemical Detection of Multidrug-Resistant Bacteria Based on Nanostructured Gold Coated ITO Electrode. *ACS Appl. Mater. Interfaces* **2014**, *6*, 11025−11031.
(30) Zhao, Y.; Xu, L.; Ma, W.; Wang, L.; Kuang, H.; Xu, C.; Kotov, N. A. Shell-Engineered Chiroplasmonic Assemblies of Nanoparticles for Zeptomolar DNA Detection. *Nano Lett.* **2014**, *14*, 3908−3913.
(31) Zhao, Y.; Xu, L.; Liz-Marzán, L. M.; Kuang, H.; Ma, W.; Asenjo-García, A.; García de Abajo, F. J.; Kotov, N. A.; Wang, L.; Xu, C. Alternating Plasmonic Nanoparticle Heterochains Made by Polymerase Chain Reaction and Their Optical Properties. *J. Phys. Chem. Lett.* **2013**, *4*, 641−647.
(32) Zhao, Y.; Xu, L.; Kuang, H.; Wang, L.; Xu, C. Asymmetric and Symmetric PCR of Gold Nanoparticles: A Pathway to Scaled-Up Self-Assembly with Tunable Chirality. *J. Mater. Chem.* **2012**, *22*, 5574−5580.
(33) Lei, J.; Ju, H. Signal Amplification Using Functional Nanomaterials for Biosensing. *Chem. Soc. Rev.* **2012**, *41*, 2122−2134.
(34) Fernandes, A. M.; Abdalhai, M. H.; Ji, J.; Xi, B. W.; Xie, J.; Sun, J.; Noeline, R.; Lee, B. H.; Sun, X. Development of Highly Sensitive Electrochemical Genosensor Based on Multiwalled Carbon Nanotubes-Chitosan-Bismuth and Lead Sulfide Nanoparticles for the Detection of Pathogenic Aeromonas. *Biosens. Bioelectron.* **2015**, *63*, 399−406.
(35) Huang, C. F.; Yao, G. H.; Liang, R. P.; Qiu, J. D. Graphene Oxide and Dextran Capped Gold Nanoparticles based Surface Plasmon Resonance Sensor for Sensitive Detection of Concanavalin A. *Biosens. Bioelectron.* **2013**, *50*, 305−310.